Journal of
Polymer Materials

Tech Science Press

DOI: 10.32604/jpm.2024.057420

ARTICLE

Poly-3,4-ethylenedioxythiophene/Polystyrene Sulfonate/Dimethyl Sulfoxide-Based Conductive Fabrics for Wearable Electronics: Elucidating the Electrical Conductivity and Durability Properties through Controlled Doping and Washing Tests

Muhammad Faiz Aizamddin[1,2,*], Nazreen Che Roslan[2], Ayu Natasha Ayub[2], Awis Sukarni Mohmad Sabere[3], Zarif Mohamed Sofian[4], Yee Hui Robin Chang[5], Mohd Ifwat Mohd Ghazali[6,7], Kishor Kumar Sadasivuni[8], Mohamad Arif Kasri[9], Muhamad Saipul Fakir[10] and Mohd Muzamir Mahat[2,*]

[1]Group Research and Technology, PETRONAS Research Sdn. Bhd., Kawasan Institusi Bangi, Kajang, 43000, Malaysia

[2]Faculty of Applied Sciences, Universiti Teknologi MARA, Shah Alam, 40450, Malaysia

[3]Kulliyyah of Pharmacy, International Islamic University Malaysia, Bandar Indera Mahkota, Kuantan, 25200, Malaysia

[4]Department of Pharmaceutical Technology, Faculty of Pharmacy, Universiti Malaya, Kuala Lumpur, 50603, Malaysia

[5]Faculty of Applied Sciences, Universiti Teknologi MARA, Kota Samarahan, 94300, Malaysia

[6]SMART RG, Faculty of Science and Technology, Universiti Sains Islam Malaysia, Nilai, 71800, Malaysia

[7]Department of Engineering, University of Cambridge, Cambridge, CB2 1PZ, UK

[8]Center for Advanced Materials, Qatar University, Doha, P.O. Box 2713, Qatar

[9]Department of Chemistry, Kulliyyah of Science, International Islamic University Malaysia, Kuantan, 25200, Malaysia

[10]Faculty of Applied Sciences, Universiti Teknologi MARA, Cawangan Johor Kampus Pasir Gudang, Masai, 81750, Malaysia

*Corresponding Authors: Muhammad Faiz Aizamddin. Email: faiz.aizamddin@petronas.com; Mohd Muzamir Mahat. Email: mmuzamir@uitm.edu.my

Received: 17 August 2024 Accepted: 31 October 2024 Published: 16 December 2024

ABSTRACT

Poly-3,4-ethylenedioxythiophene: polystyrene sulfonate (PEDOT/PSS) has revolutionized the field of smart textiles as an advanced conductive polymer, offering an unprecedented combination of high electrical conductivity, solution processability, and mechanical conformability. Despite extensive research in PEDOT/PSS-coated fabrics over the past decade, a critical challenge remains in finding the delicate balance between enhanced conductivity and washing durability required for real-world wearable applications. Hence, this study investigates the electrical conductivity and durability properties of PEDOT/PSS-based conductive fabrics for wearable electronics. By carefully controlling the doping concentration of dimethyl sulfoxide (DMSO), an optimal conductivity of $8.44 \pm 0.21 \times 10^{-3}$ S cm^{-1} was achieved at 5% DMSO. Durability was assessed through simulated washing tests of up to 30 cycles following standardized protocols. Although the fabric's conductivity decreased from 10^{-3} to 10^{-4} S cm^{-1} after the 5th wash, it stabilized at approximately $\sim 5.67 \pm 0.05 \times 10^{-4}$ S cm^{-1} beyond the 30th cycle. These findings demonstrate the fabric's ability to retain its electrical properties under repeated washing, making it highly suitable for long-term use in wearable electronics. A range of characterization techniques—including attenuated total reflectance–Fourier transform infrared spectroscopy, Raman analysis, scanning electron microscopy–energy dispersive X-ray, X-ray diffraction, electrochemical impedance spectroscopy, and tensile testing—were employed

to analyze the fabric's functional groups, morphology, crystallinity, conductivity, and mechanical properties. The results validate the robustness and applicability of PEDOT/PSS/DMSO fabrics for reliable performance in wearable electronic applications.

KEYWORDS

Conductive fabric; electrical conductivity; durability; PEDOT/PSS; wearable electronic

1 Introduction

Wearable electronics have received tremendous attention over the past few years, mainly in the electronic industry and healthcare, which strives to stimulate signals like heart rate [1], body motion [2] and blood pressure [3]. This technology offers additional insights on physiological status with personalised use and real-time feedback for consumers. According to the statistical data by "Statista-wearable-electronics", almost half a billion wearable electronics were utilised in 2020. This trend is influenced by the development of 5G technology and artificial intelligence [4]. Wearable electronics can be implanted on the skin, and integrated into clothing articles, body attachments and insertion [5]. Wearable devices have gradually assumed the form of commercial clothing, integrated clothing, printed fabric and intelligent fabric devices (Fig. 1a). Over the years, tremendous advances in electronic, biocompatible materials and nanomaterials have led to the development of wearable devices in fabric such as heart monitor, sweat sensor, strain sensor, electrocardiogram (ECG) and data storage (Fig. 1b) [6,7]. These practical hands-free devices have enhanced electronic properties. Conductive materials like metal [8,9], carbon [10,11] and conducting polymers (CPs) can be integrated into the fabric [12,13].

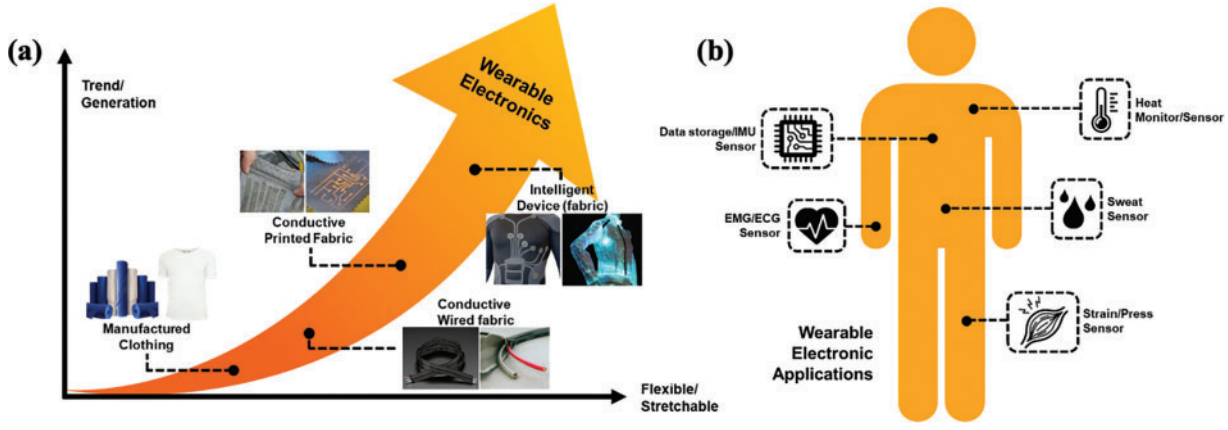

Figure 1: Schematic illustration on the (a) trends of wearable electronics and (b) their potential applications

CPs, such as polyaniline (PANI) [14–17], polypyrrole (PPy) [18] and poly-3,4-ethylenedioxythio phene: polystyrene sulfonate (PEDOT/PSS), offer new possibilities for conductive fabric materials [19,20]. Among them, PEDOT/PSS offers solution processability, excellent flexibility, biocompatibility and long-term stability. Ironically, this CP has not been categorised as a primary candidate to manufacture conductive fabrics [21,22]. Also known as a conjugated polymer, PEDOT/PSS' electrical conductivity can be amplified with doping. The doping requires the addition of organic reagents, such

as dimethyl sulfoxide (DMSO), which promotes for the charge balancing on the surface structure of PEDOT/PSS [23]. However, achieving its optimal conductivity remains a significant challenge. Despite the vast reports on the conductivity enhancement of PEDOT/PSS fabrics using dopants, the exact amount of dopant concentration required for reliable and consistent electronic properties is still unclear. In particular, the electronic stability and durability of the PEDOT/PSS fabric are critical for wearable electronics, which are subjected to frequent washing and stretching [24–26]. The mechanical scrubbing and chemical reactions that occur during the washing obstacle can remove the conductive coating, leading to conductivity decay. In addition, the poor mechanical properties of conductive fabrics after washing also contribute to the challenges of creating excellent wearable electronics [27,28]. Therefore, it is essential to critically investigate the optimisation of conductivity and durability properties of conductive fabrics to ensure their suitability for real-world applications.

To address this issue, the present study highlighted the optimisation of DMSO to achieve a maximum conductivity value of PEDOT/PSS/DMSO fabric. The durability of PEDOT/PSS/DMSO fabric was demonstrated for up to 30 simulated washing cycles following standard practices. Before this, the preparation of PEDOT/PSS including its polymerisation and doping was thoroughly discussed. The functional group of each compound and optimisation of electrical conductivity of PEDOT/PSS fabric were confirmed by attenuated total reflectance-Fourier transform infrared spectroscopy (ATR-FTIR) collaborated with Raman analysis and electro impedance spectroscopy (EIS), respectively. Sample characterisations were performed with scanning electron microscopy-energy dispersive X-ray (SEM-EDX), X-ray diffraction analysis (XRD) and tensile test to determine the morphological surface, crystallinity, and mechanical properties of PEDOT/PSS/DMSO fabric, respectively.

2 Materials and Methods

2.1 Chemicals and Reagents

3,4-Ethylenedioxythiophene (EDOT) (M_w = 142.18 g/mol), poly (styrene sulfonate) (PSS) solution (M_w = ~75000, 18 wt.% in H_2O), ammonium persulfate ($(NH_4)_2S_2O_8$) (reagent grade, 98%), dimethyl sulfoxide (DMSO) (reagent plus, 99%) and anhydrous sodium carbonate (Na_2CO_3) were purchased from Sigma Aldrich (St. Louis, MO, USA). A large-scale size of bare polyester fabric-knitted type in 50 cm × 50 cm was purchased from Jakel Trading Sdn. Bhd. (Shah Alam, Malaysia).

2.2 Preparation and Optimisation of PEDOT/PSS Fabric

PEDOT/PSS was synthesised through a chemical oxidation method, which some part was inspired from previous finding [29]. 0.05 mL EDOT was mixed with 0.08 mL PSS in a 1:1.6 ratio with the addition of 10 mL deionised water. The solution was stirred for 30 min at room temperature to acquire EDOT: PSS solution. Here, EDOT serves as the monomer for creating conductive polymers, PSS acts as a dopant and stabilizer to enhance conductivity and solubility, and deionized water serves as a solvent to ensure even mixing and prevent interference from unwanted ions. A 1:2 ratio of ammonium persulfate was added to the solution to initiate the polymerisation of PEDOT. The solution was stirred for another 2 h until its colour changed to dark blue, indicating its complete polymerisation. A filtration process was employed to purify the PEDOT/PSS by-product. Specifically, the Grade 1 qualitative filter paper is used (11 µm pore size) to remove larger impurities, particulate matter, and aggregates from the solution of PEDOT/PSS. Following this, a variation concentration of DMSO from 1, 3, 5, 7 and 9 volume percentages (v/v%) was prepared and added to the 10 mL PEDOT/PSS solution. The solution was stirred for 2 h using a magnetic stirrer at room temperature, set to a moderate stirring speed of 100 rotations per minute, to ensure complete mixing and uniform distribution of the components. The PEDOT/PSS fabric was fabricated with the immersion technique. Bare polyester fabrics cut to sizes of 5 cm × 5 cm, 20 cm × 7.5 cm and 10 cm × 4 cm were submerged in 12 mL pristine

PEDOT/PSS solution for 30 min. The pristine PEDOT/PSS fabric acted as the control sample. The method was repeated with 1, 3, 5, 7 and 9 v/v% DMSO/PEDOT/PSS fabric. All samples were dried and stored at room temperature.

2.3 Characterisation of PEDOT/PSS Fabric

The IR spectra were studied with attenuated total reflectance-Fourier transform infrared (ATR-FTIR) spectroscopy (Perkin-Elmer Spectrum 100, London, UK). The analysis was performed at room temperature with ambient humidity. The spectra were recorded from 450 to 4000 cm^{-1} at 20 kHz frequency with a resolution of 16 cm^{-1}. Each spectrum was recorded with a mirrored diamond surface under spectroscopic circumstances. The spectrum was analysed with BIO-RAD WIN-IR PRO software (version 10, Perkin-Elmer, Ltd., London, UK) to identify the functional group components within the PEDOT/PSS fabric. Additionally, Raman analysis (brand: Renishaw, model: In via Raman) was used to support the FTIR analysis.

The electrical conductivity of PEDOT/PSS fabric was measured with electrochemical impedance spectroscopy (EIS) (model: HIOKI 3532-50 LCR-HI Tester, HIOKI E. E. Corporation, Nagano, Japan). The analysis was performed at room temperature with a frequency range of 100 Hz to 1000 kHz. PEDOT/PSS fabric was clamped between two copper electrodes with a 1 cm diameter. The thickness of the fabric was measured beforehand with a digital thickness gauge. An average of three measurements was recorded. Conductivity measurements were derived from the following expression Eq. (1) [30,31]:

$$\sigma = L/(R_b \times A) \quad (1)$$

where σ is conductivity, R_b is the bulk resistance measured by the instrument, L is the sample thickness, and A is the contact surface area (1 cm) of the electrode with the fabric.

The surface morphology of PEDOT/PSS fabrics was observed with scanning electron microscopy (SEM) (model: SNE-4500M Plus Tabletop SEM, SEC Co., Ltd., Suwon-Si, Republic of Korea). Before this observation, a ~10 nm gold (Au) film was sputtered on the samples to improve the image's resolution. The samples were cut with a razor blade before capturing the images with magnifications ranging from 200× to 800×. The samples' elemental compositions and mapping were analysed with energy dispersive X-ray (EDX) (AZtecOne, Oxford Instruments Group, Oxfordshire, England, UK).

The crystallinity of the PEDOT/PSS fabric was measured with X-ray diffraction (XRD) analysis (model: PANalytical X-Pert Pro XRD Machine, PANalytical B. V., Almelo, The Netherlands). The 2θ range was 0° to 60°. The parameter was configured to a 1-h exposure and Cu-Kα radiation (λ = 0.15418 nm) at 40 kV and 40 mA, from 0° to 60° in a continuous mode. The XRD pattern was analysed with X'pert Highscore and X'pert Plus software (source: PANalytical B. V., Almelo, The Netherlands) to identify the properties of the PEDOT/PSS fabric. The percentage of crystallinity (X_c) was calculated by the Hinrichen method Eq. (2) [32]:

$$X_c = A_c/A_a \times 100 \quad (2)$$

where A_c is the total area of crystalline peaks, and A_a is the total area of amorphous peaks.

PEDOT/PSS fabric's mechanical strength properties were analysed with a universal strength tester machine (model: Tenso Lab 5000, MESDAN S.p.A, Puegnago del Garda (BS), Italy). PEDOT/PSS fabric in 20 cm × 7.5 cm was prepared and tested in warp and weft structures. 300 mm/min rate of transverse and 5 kN load force was used for each sample. Tensile strength and percentage elongation at break were recorded from the analysis.

2.4 Simulated Washing Test

The washability of the PEDOT/PSS fabric was evaluated to determine its durability in 30 washing cycles (machine model: Washing Fastness Tester UI-TX58, Unuo Instruments Co. Ltd., Quanzhou, China). The conductivity value of the sample was recorded in each washing cycle. This simulated washing test complied with EN ISO 105 C06. Prior to this, the soap solution was prepared by mixing 5 g standard soap with 2 g anhydrous sodium carbonate (Na_2CO_3) in 1 L distilled water. The solution was heated to 60°C ± 2°C. The optimized 5v/v% DMSO/PEDOT/PSS fabric in 10 cm × 4 cm was placed in the solution at a 1:50 solution ratio and washed for 30 min. Then, the samples were rinsed with distilled water and dried at room temperature.

3 Results and Discussion

3.1 Preparation and Optimisation of PEDOT/PSS/DMSO Fabric

PEDOT/PSS solution was successfully synthesised through chemical oxidation. The hydrophobicity nature of ethylenedioxythiophene (EDOT) has been a challenge in its synthesis processability [33]. The primary doping of poly(styrenesulfonate) (PSS) was adopted in this study to address the issue. PSS is a common material to stabilises EDOT monomer through ionic bonding and facilitate the solution processability [34]. The presence of PSS as counter-ions is portrayed as the charge balancing and keeps the PEDOT segment dispersed in an aqueous solution [35]. The synthesis of PEDOT/PSS was initiated with the addition of PSS into the EDOT monomer solution. Ammonium persulfate (APS) was introduced as an oxidant to trigger polymerisation.

The chemical oxidation of PEDOT/PSS can be broken down into three steps: disassociation of oxidant, oxidation of EDOT, and doping with PSS. In the first step, APS (oxidant and initiator) dissociates into sodium ions and a persulfate ion. In this condition, persulfate ions disintegrate into sulphate radicals in an aqueous solution [29]. In the second step, the EDOT monomer is oxidised into an EDOT cation (+) by the sulphate radical, leading to the formation of sulphate anions (−). These conditions promoted the polymerisation of PEDOT (coupling of EDOT chains). The PSS and sulphate ions interact with the oxidised PEDOT chains, and these constituents are linked to each other. The chemical structure in the synthesis process is visualised in Fig. 2a.

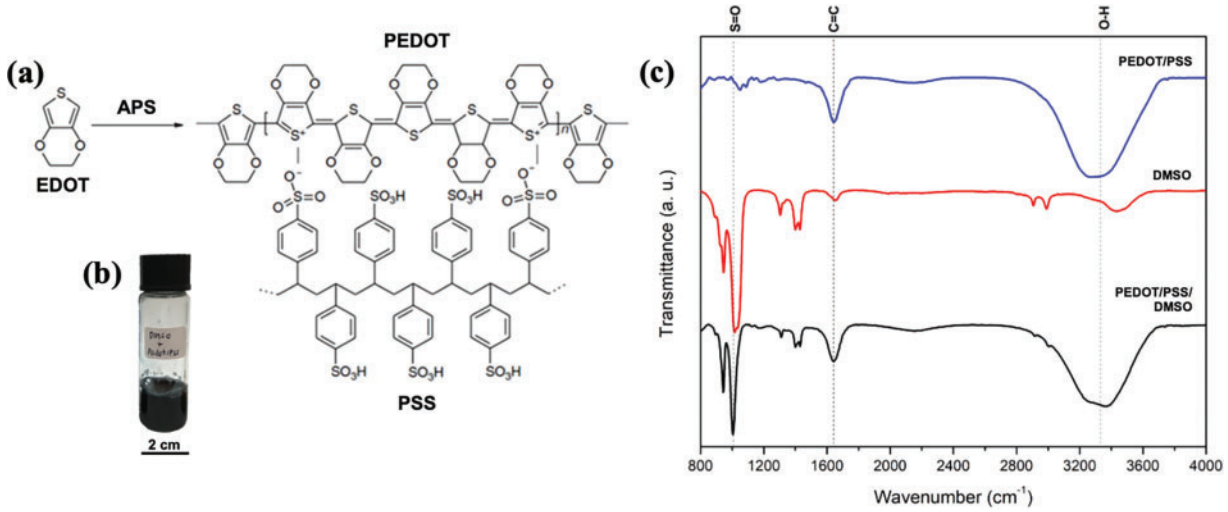

Figure 2: The chemical structure, physical appearance, and FTIR spectrum of PEDOT/PSS, (a) Chemical structure of synthesised PEDOT/PSS. (b) Physical appearance of PEDOT/PSS/DMSO solution. (c) The FTIR spectrum of pristine PEDOT/PSS, DMSO and PEDOT/PSS/DMSO solution

Several studies have reported that the low electrical conductivity of pristine PEDOT/PSS is a major limitation, restricting its potential for wearable electronic applications [36–38]. In this study, dimethyl sulfoxide (DMSO) was utilised as the secondary dopant to enhance the electrical conductivity of PEDOT/PSS. The dark blue colour of the PEDOT/PSS/DMSO solution is shown in Fig. 2b. During its synthesis, PEDOT was combined with the PSS chain via columbic interaction, due to the attraction between cation PEDOT (+) and anions PSS (−) (Fig. S1a) [39]. The attachment of PEDOT and PSS chains produced a coiled formation, which distressed the charge transfer mobility between PEDOT inter-chains. The addition of DMSO could remove some of the PSS chains and construct the linear chain of PEDOT, concurrently [40,41]. Therefore, the efficiency of charge between PEDOT intergrains could be improved.

In this case, DMSO played an essential role in influencing electrical conductivity. It promoted a stable hydrogen bonding between the oxygen atom (O) from DMSO and hydrogen (H) from PSSH with van der Waals forces. Consequently, a certain amount of PSSH was dissolved in the DMSO (Fig. S1b) [42]. According to Zhu et al. [43], the PSSH-solvent interaction represents two significant effects on the PEDOT/PSS grains mechanism; (i) chain extension from coil structure and phase separation of the PSSH shell, and (ii) charge screening and phase separation of PSS-PEDOT. Both conditions contributed to the removal of PSSH. When PSSH was removed, the connectivity between PEDOT grains was reinforced. When this situation took place, the charge could move swiftly between the PEDOT-to-PEDOT intergrains.

ATR-FTIR analysis was employed to evaluate chemical structural changes in the PEDOT/PSS solution (Fig. 2c). Several absorption peaks were recorded for pristine PEDOT/PSS, DMSO and PEDOT/PSS/DMSO solution. The bands at 1643.52 cm^{-1} corresponded to the peaks of the C = C stretching vibration of the thiophene ring of PEDOT. This peak confirmed the presence of PEDOT in the solution and suggested a successful formation of PEDOT in the polymerisation reaction [44,45]. Moreover, the peaks at 1012.92 cm^{-1} and ~3328.18 cm^{-1} corresponded to the sulfonate (S = O) group of DMSO and hydroxyl group (O-H) of PSS, respectively [46,47]. The existence of the S = O peak in the PEDOT/PSS/DMSO solution was proof of successful doping without any degradation to PEDOT. In contrast, the decrement of intensity at the hydroxyl band pointed to the removal of PSS upon doping with DMSO, which is consistent with the principle explained in PSSH-solvent interaction as clarified in Fig. S1b and other previous study [48].

In the understanding of the PEDOT/PSS grains mechanism and its structural confirmation, the enhancement of electrical conductivity could be improved by doping with DMSO. However, the stability of the electrical conductivity and prospecting their optimum values are highlighted as the major issues. Five concentrations of DMSO in 1, 3, 5, 7 and 9 v/v% were prepared for doping in PEDOT/PSS. A facile immersion technique was performed to fabricate PEDOT/PSS/DMSO onto the fabric. Polyester (PES) fabric was selected as the fabrication medium of fabrication due to its flexibility, excellent strength and exceptional absorption rate [49].

Bare PES fabric was immersed in each variation of PEDOT/PSS/DMSO solution in a 1:6 volume ratio for 30 min at room temperature. This approach maximised the absorption rate of PEDOT/PSS/DMSO solution onto the fabric through the promotion of hydrogen bonding (as illustrated in Fig. S2) [50]. The fabricated PEDOT/PSS/DMSO fabric was dried at room temperature for 24 h. The physical appearance of the PEDOT/PSS/DMSO-treated fabric is shown in Fig. 3, with Fig. 3a representing the bare PES fabric (without PEDOT/PSS), Fig. 3b as the control, and Fig. 3c–g depicting samples with increasing DMSO concentrations. A noticeable transition in color is observed across the samples, where the fabric color shifts from dark blue to light blue as the concentration of DMSO increases. This color transition is closely related to the electronic and structural changes in the PEDOT system induced by DMSO. PEDOT is a conjugated polymer whose optical properties

are governed by its oxidation state, often referred to as its doping level. In its neutral, undoped state, PEDOT is transparent or light blue, while in its oxidized state (doped state), it appears dark blue due to the presence of polarons, which are localized charge carriers. As the concentration of DMSO increases, it promotes structural reorganization within the PEDOT matrix, specifically enhancing the phase separation between the conductive PEDOT-rich domains and the insulating PSS-rich domains. This reorganization, facilitated by DMSO, significantly improves the electrical conductivity of PEDOT by reducing Coulombic interactions between PEDOT and PSS, leading to a higher degree of chain alignment and π-π stacking in PEDOT domains. These structural changes correspond to a gradual increase in the oxidation level of PEDOT, as more charge carriers become delocalized along the polymer backbone. As a result, the absorption spectrum shifts, reducing absorption in the visible region, which causes the fabric to appear lighter in color. Levasseur et al. [51] confirmed that this color change is indicative of the transition from a lower oxidation state (dark blue), where the polymer has a high concentration of localized charge carriers (polarons), to a higher oxidation state (light blue), where the polymer exhibits fewer polarons and more bipolaron formation. The addition of DMSO increases the effective doping of PEDOT by enhancing ion exchange and promoting a more conductive and optically transparent at higher concentrations.

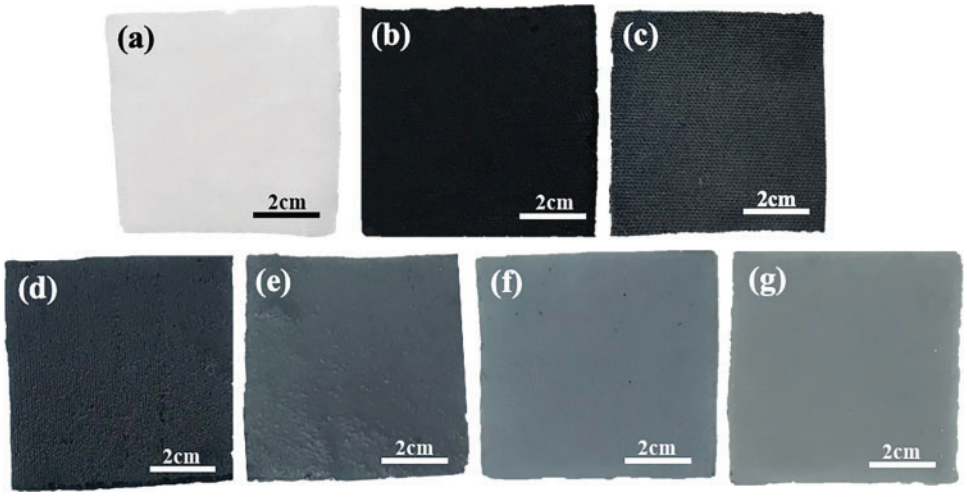

Figure 3: Physical appearance of (a) bare PES fabric, (b) pristine PEDOT/PSS, (c) 1% DMSO/PEDOT/PSS, (d) 3% DMSO/PEDOT/PSS, (e) 5% DMSO/PEDOT/PSS, (f) 7% DMSO/PEDOT/PSS and (g) 9% DMSO/PEDOT/PSS fabrics

3.2 Characterisation of PEDOT/PSS Fabric

The conformational chemical structure and functional groups of PEDOT/PSS/DMSO fabrics are displayed in Fig. 4a. The chemical structure of the C = C thiophene ring was attributed to the existence of PEDOT, while the hydroxyl group (O-H) were attributed to PSS chain [52]. The peaks at 1008.82 cm^{-1} signalled the successful doping process of the sulfonate group (S = O) of DMSO with PEDOT/PSS fabric. The peak intensity increases according to the level of doping concentration of DMSO. The C = C of thiophene ring was detected at 1643.58, 1643.58, 1643.59, 1643.61, 1643.63, and 1643.65 cm^{-1} for pristine PEDOT/PSS fabric, 1%, 3%, 5%, 7% and 9% DMSO/PEDOT/PSS fabrics, respectively. These peaks were attributed to the presence of PEDOT in the fabric [53]. The peak intensity was consistent considering that there was no significant effect in PEDOT upon doping with DMSO. Also, it is worthwhile to note that the C = C stretching of quinoid PEDOT is shifted to the higher wavenumber from 1634.45 to 1645.49 cm^{-1} (Fig. 4b) after increasing the concentration

of DMSO. Raman spectroscopy was further used to confirm the symmetrical bond at the molecular level of PEDOT (Fig. 4c). The major characteristic peaks of pristine PEDOT/PSS fabric ranged from 1608.93 to 1722.20 cm^{-1}. For pristine PEDOT/PSS fabric, these two principal peaks are attributed to C_α–C_α' inter-ring stretching vibration and $C_\alpha = C_\beta$ symmetric stretching vibration, respectively. Upon doping with DMSO, the peak was red-shifted to the 1611.13 and 1725.85 cm^{-1}, respectively, which involved the transformation of the benzenoid structure into the quinoid structure of PEDOT [45]. Other studies reported that the benzenoid structure may be the favourite structure of coil confirmation, while quinoid may assist the linear or an expended coil structure [54]. Moreover, the band shifting at 1722.20 to 1725.85 cm^{-1} is related to the doping-induced peak, which is split from the asymmetrical $C_\alpha = C_\beta$ stretching mode band and consistent with the oxidized state of PEDOT/PSS. Through these structural changes, the linear or coil-expanded conformation would possess almost the same plane, which grants the delocalization of electrons and increases the electrons' mobility. Finally, the hydroxyl group (O-H) bending vibration was attributed to the hydroxyl group of PSS, which transpired at a range of ~3320.86 cm^{-1} wavenumber. The intensity of these bands decreased proportionally with the concentration of DMSO in the PEDOT/PSS fabric. Additionally, the existence of these bands was proof of the removal of PSS upon doping with DMSO. As mentioned by Abel et al. [55], the presence of DMSO could potentially bind with the SO_3 group in PSS chains via hydrogen bonding and disturb the main structure of PEDOT and PSS. Therefore, this condition leads to the removal of certain PSS and provides an extended coil to the linear chain of PEDOT/PSS.

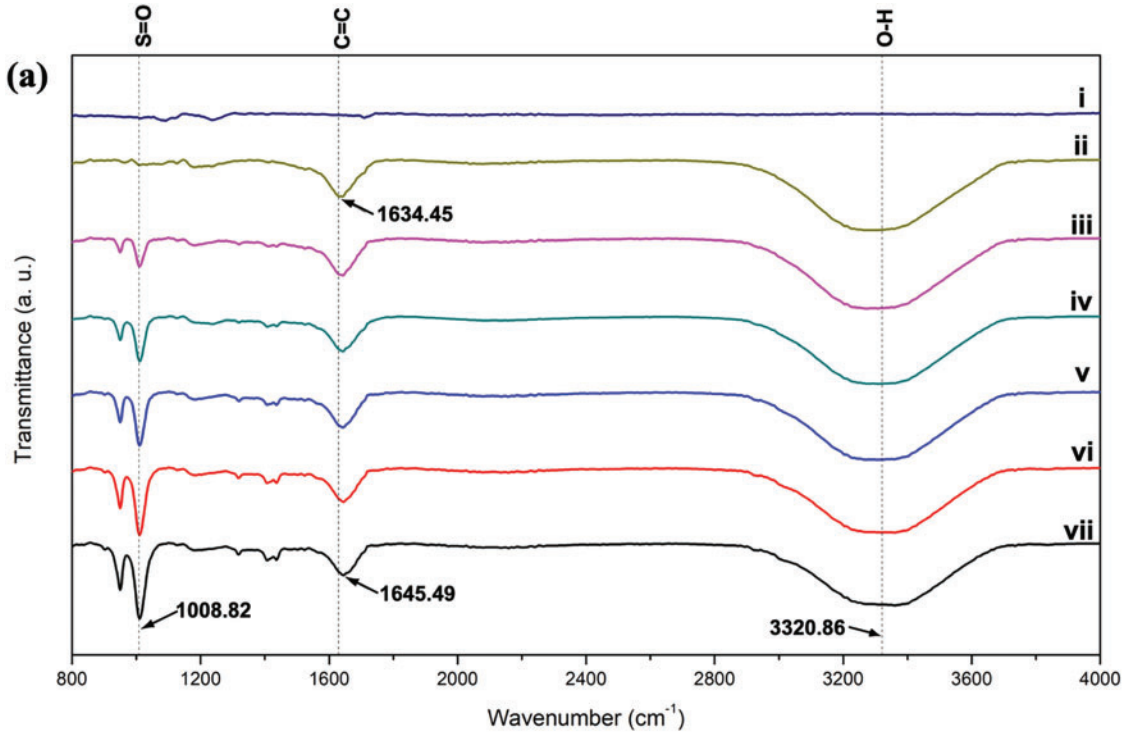

Figure 4: (Continued)

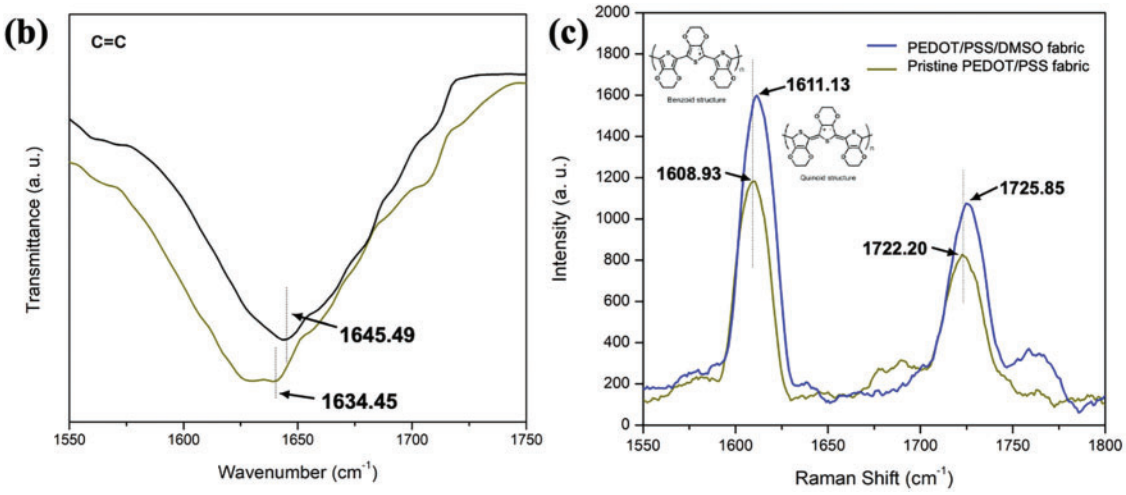

Figure 4: Recorded results for (a) FTIR spectra of i-PES fabric, ii-pristine PEDOT/PSS fabric, iii-1% DMSO/PEDOT/PSS, iv-3% DMSO/PEDOT/PSS, v-5% DMSO/PEDOT/PSS, vi-7% DMSO/PEDOT/PSS and vii-9% DMSO/PEDOT/PSS fabrics. (b) C = C spectrum of all samples. (c) Raman spectroscopy of pristine PEDOT/PSS fabric and PEDOT/PSS/DMSO fabric

SEM analysis was utilised to observe the morphological changes of bare PES, pristine PEDOT/PSS and PEDOT/PSS/DMSO fabric. This technique was combined with EDX analysis to determine the elemental composition of the fabric. Based on Fig. 5a, bare PES fabric had a clear fibre structure due to the absence of PEDOT/PSS. On the contrary, pristine PEDOT/PSS fabric and PEDOT/PSS/DMSO fabric (Fig. 5b–g) displayed a homogenous fibre surface after fabrication. The addition of DMSO onto PEDOT/PSS fabric has significantly enhanced the PEDOT/PSS solution's wetting properties, leading to improved coverage and smoother surfaces when deposited on a fabric. It is worth noting that the fabric was successfully coated with PEDOT/PSS through the immersion technique. The entire surface of the yarn (bundle of fibre) was covered with fluid-like PEDOT/PSS and held together between the fibre. Moreover, there was a deeper penetration of the fluid in the fibre of pristine PEDOT/PSS fabric and PEDOT/PSS/DMSO fabric. Nevertheless, there was no morphological difference between pristine PEDOT/PSS fabric, 1%, 3% and 5% DMSO/PEDOT/PSS fabric (Fig. 5b–e). EDX-mapping analysis illustrated the distribution of sulphur (S), carbon (C) and oxygen (O) that existed on the fabric (Fig. 5c). The elemental compositions of all samples are presented in Table 1.

A saturated fluid-like PEDOT/PSS was observed when the concentration of DMSO was increased to 7% and 9% (Fig. 5f,g). The fluid-like PEDOT/PSS was subjected to strain within the fiber, leading to aggregation, uneven distribution of PEDOT/PSS, and a rougher surface area. Despite these effects, certain underlying fiber bundles remained visible. This saturated PEDOT/PSS fibre had lower conductivity when compared to unsaturated fibre [23]. The saturated phase of PEDOT/PSS was brittle with greater resistance to electrical charge [36].

From Table 1, the S element in PEDOT/PSS/DMSO fabric was increased upon doping with a higher concentration of DMSO. S element was absent in bare PES fabric, confirming the absence of DMSO in the fabric. According to Kanjana et al. [56], C and O elements were highlighted as the composition of PEDOT and PSS, respectively. There were significantly no composition changes in PEDOT, assuming there was no elemental effect upon doping with DMSO. In contrast, the decrement composition of PSSH was dissolved in the DMSO and construct a saturated fluid was constructed [57].

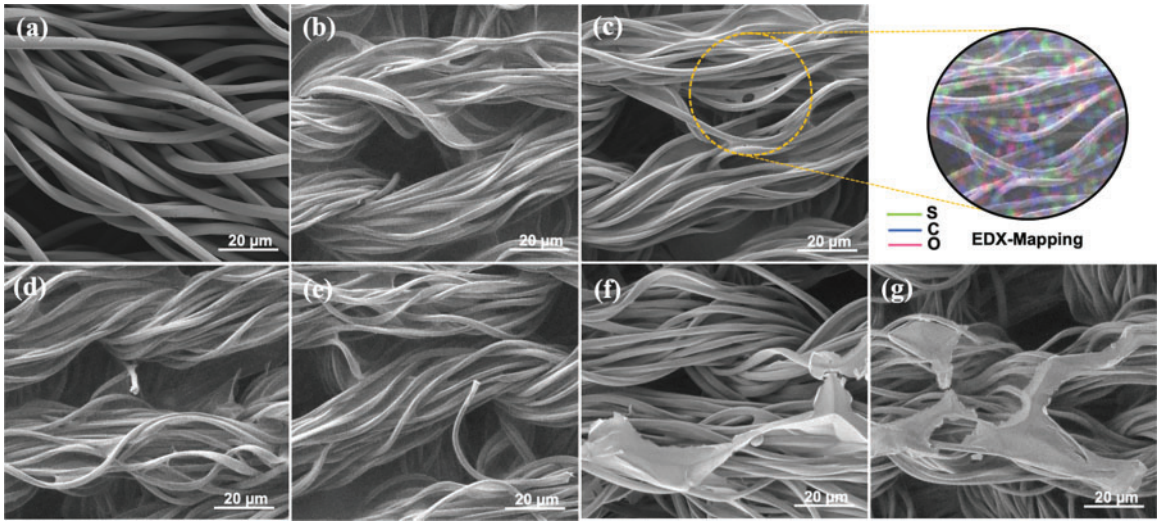

Figure 5: Morphological images of (a) bare PES fabric, (b) pristine PEDOT/PSS fabric (c) 1% DMSO/PEDOT/PSS fabric with EDX-mapping analysis, (d) 3% DMSO/PEDOT/PSS fabric, (e) 5% DMSO/PEDOT/PSS fabric, (f) 7% DMSO/PEDOT/PSS fabric and (g) 9% DMSO/PEDOT/PSS fabric

Table 1: Elemental composition of bare PES fabric, pristine PEDOT/PSS fabric and PEDOT/PSS/DMSO fabric from EDX analysis

	Element composition (%)		
	S	C	O
Bare PES fabric	NIL	88.23	11.77
Pristine PEDOT/PSS fabric	10.11	65.63	24.26
1% DMSO/PEDOT/PSS fabric	15.16	65.31	19.53
3% DMSO/PEDOT/PSS fabric	17.16	65.22	17.62
5% DMSO/PEDOT/PSS fabric	18.36	65.28	16.36
7% DMSO/PEDOT/PSS fabric	20.12	65.19	14.69
9% DMSO/PEDOT/PSS fabric	21.83	65.19	12.98

In the previous section, PEDOT/PSS/DMSO fabrics were incorporated with DMSO as the dopant. The concentration of DMSO impacted electrical conductivity. Therefore, electro-impedance spectroscopy (EIS) analysis was performed to determine the electrical conductivity of those fabrics while identifying an optimum DMSO condition. The values of conductivity are presented in Table 2.

It is worth noting that pristine PEDOT/PSS fabric and PEDOT/PSS/DMSO fabric fell within the range of semiconductive and conductive states of polymer (10^{-7} to 10^{6} S cm^{-1}) [58,59]. Even without the dopant, pristine PEDOT/PSS fabric ($9.10 \pm 0.01 \times 10^{-6}$ S cm^{-1}) could carry an electrical charge with minimal value compared to PEDOT/PSS/DMSO fabric. Upon doping with DMSO, the conductivity was altered according to the different concentrations of DMSO. The conductivity trend of PEDOT/PSS/DMSO fabric is shown in Fig. 6.

Table 2: The conductivity values of PEDOT/PSS fabrics with various concentrations of DMSO

Doping condition	Concentration of DMSO (%)	Conductivity (S cm^{-1})
Bare PES fabric	–	NIL
Pristine PEDOT/PSS fabric	0	$9.10 \pm 0.01 \times 10^{-6}$
PEDOT/PSS/DMSO fabric	1	$4.87 \pm 0.04 \times 10^{-5}$
	3	$7.88 \pm 0.13 \times 10^{-4}$
	5	$8.44 \pm 0.21 \times 10^{-3}$
	7	$2.60 \pm 0.15 \times 10^{-3}$
	9	$3.87 \pm 0.14 \times 10^{-4}$

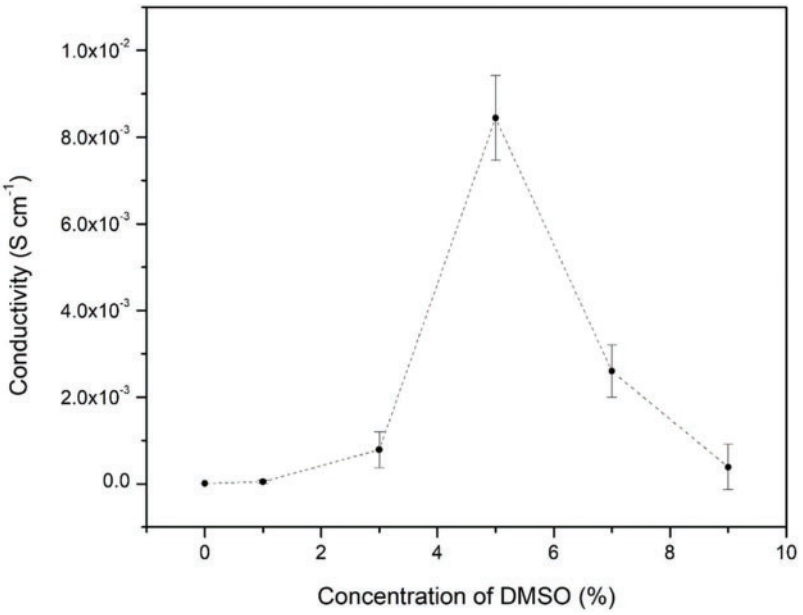

Figure 6: Conductivity trend of PEDOT/PSS fabric with different concentrations of dopant

Based on Fig. 6, there was a significant spike from pristine PEDOT/PSS fabric to 3.0% of DMSO/PEDOT/PSS fabric. This finding suggested a relationship between varying concentrations of DMSO and the conductivity of PEDOT/PSS fabric. Theoretically, the incorporation of DMSO as the dopant provides the compact coil structure of PEDOT/PSS becoming more elongated and able to facilitate the transportation of charges. This condition augmented the charge carrier mobility within the fabric [43]. The addition of 3% to 5% DMSO produced a maximum conductivity value ($8.44 \pm 0.21 \times 10^{-3}$ S cm^{-1}) in PEDOT/PSS fabric. In this state, charge transport was likely the fastest along the PEDOT/PSS backbone due to the improvement of charge carrier transport in the fabric. According to previous studies [13,59] the resulting value was considered in the semiconductor range measurement of polymer (10^{-6} to 10^{6} S cm^{-1}), which embarked as the promising value in wearable electronics applications. Moreover, this value was closely engaged with other CPs based on fabric in previous studies as summarised in Table 3.

Table 3: Conductivity values of CPs-based fabric achieved in previous studies

Fabric	CP	Dopant	Conductivity (S cm^{-1})	Ref.
Cotton	PANI	0.9 wt% *p*-toluene sulfonic acid	8.85×10^{-3}	[60]
Polyester	PANI	30% phytic acid	2.15×10^{-4}	[60]
Cotton	PANI	0.9% hydrochloric acid	1.57×10^{-2}	[17]
Nanocellulose	PPy	–	4.0×10^{-7}	[61]
Polyester	PEDOT/PSS	6 v/v% ethylene glycol	4.06×10^{-3}	[62]
Polyurethane	PEDOT/PSS	Sodium dodecylsulfate	2.08	[63]
Cotton	PEDOT/PSS	Sodium dodecylsulfate	4.17	[63]
Polyamide nylon	PEDOT/PSS	Glycerol	7.14 ± 1.61	[64]
Polyester fabric	PEDOT/PSS	5% DMSO	8.44×10^{-3}	This work

The electrical conduction of PEDOT/PSS/DMSO grain formation can be explained in 3 phases (as illustrated in Fig. S3) [65]. In the 1st phase, the addition of DMSO into PEDOT/PSS reduced and segregated the PSS shell along PEDOT's surface. It causes the cohesion between PEDOT grains and the increment in their size. The cohesion of PEDOT grains transpired when the dopant was weakened, and the Coulombic Attraction between PEDOT and PSS was compromised. Due to this condition, some PEDOT grains clumped together to form bigger grains (2nd phase). Eventually, the coil structure of PEDOT grains changed into a linear structure and induced the conductivity of PEDOT/PSS in the charge carrier pathway (3rd phase). The rise of dopant concentration potentially amplified the conductivity of PEDOT/PSS. Nevertheless, the conductivity dropped to $3.87 \pm 0.14 \times 10^{-4}$ S cm^{-1} after the dopant was increased to 9%. The decrement is reported by one order of magnitude from the 5% dopant. It could be proposed that the conductivity of PEDOT/PSS had reached a degree of saturation after doping with 5%, 7% and 9% DMSO. A saturation condition is defined as an electrical charge that resists mobility which causes an obstacle to electrical conductivity in PEDOT/PSS [66]. This study provided evidence that a 5% DMSO concentration is the ideal dopant concentration to achieve maximum conductivity in PEDOT/PSS fabric. As a result, 5% DMSO/PEDOT/PSS was selected as the candidate in the following tests.

One of the major variables that impact the electrical conductivity of PEDOT/PSS fabric is its crystallisation characteristic. This characteristic informs the stacking tightness of polymer molecules [67]. An organic solvent such as DMSO can improve the crystallinity properties of the PEDOT/PSS structure. In turn, this improvement can promote charge transportation electrical conductivity of PEDOT/PSS. XRD analysis was performed to compare the diffraction angle of pristine PEDOT/PSS fabric and the optimised PEDOT/PSS/DMSO fabric. This analysis was crucial to validate the polymer alignment of PEDOT/PSS induced by DMSO.

For pristine PEDOT/PSS fabric (Fig. 7a), two (2) characteristic peaks were observed at $2\theta = 17.8°$ and 25.8° which can be indexed to the (113) and (311) plane of hexagonal structure [68]. The 2θ value corresponds to the d-spacing of approximately 4.95 and 3.47Å. The low-angle reflections at $2\theta = 17.8°$ show the lamellar stacking distance of two distinct alternate ordering of PEDOT and PSS, whereas the high-angle reflections at $2\theta = 25.8°$ show the amorphous halo of PSS and the interchain planar ring-stacking distance of PEDOT. As illustrated in Fig. 7b, the lamellar stacking was in the perpendicular line with the substrate, attached between the edge of PEDOT/PSS chains and between two planes. The distance between the two planes was significantly higher, thus causing the slow interaction transport and induced lower electrical charge mobility [57]. On the contrary, the

π-π stacking structure is defined as the chain interaction between PEDOT/PSS that was parallel to the substrate. According to Lai et al. [69], π-π stacking also symbolised the presence of electrostatic and direct interaction of PEDOT/PSS chains in the conjugated polymer system. Therefore, these so-called "face-on" or in-plane orders of PEDOT/PSS chains showed fast electrons hopping transportation along the polymer backbone. XRD spectrum (Fig. 7c) revealed that PEDOT and PSS became more crystalline after introducing DMSO as a dopant. The peak intensity increased dramatically from 57.89% to 66.31% crystallinity index as calculated in Table 4. The higher value of the crystallinity index is due to the rearrangement of the PEDOT/PSS structure. This circumstance was consistent with the change in the PEDOT structure from coiled to extended chain conformations and lamellar stacking converted to the π-π stacking arrangement [70]. The rearrangement and conformational changes of the PEDOT structure result in the easier path of electron charge movement and thus be the reason for electrical conductivity improvement. In addition, there are some sharp peaks appeared for the doped PEDOT/PSS fabric suggesting the amorphous structure of PEDOT/PSS reformed to an ordered arrangement [71]. Meanwhile, $2\theta = 22.8°$ attributed to the crystallinity of PES fabric [72].

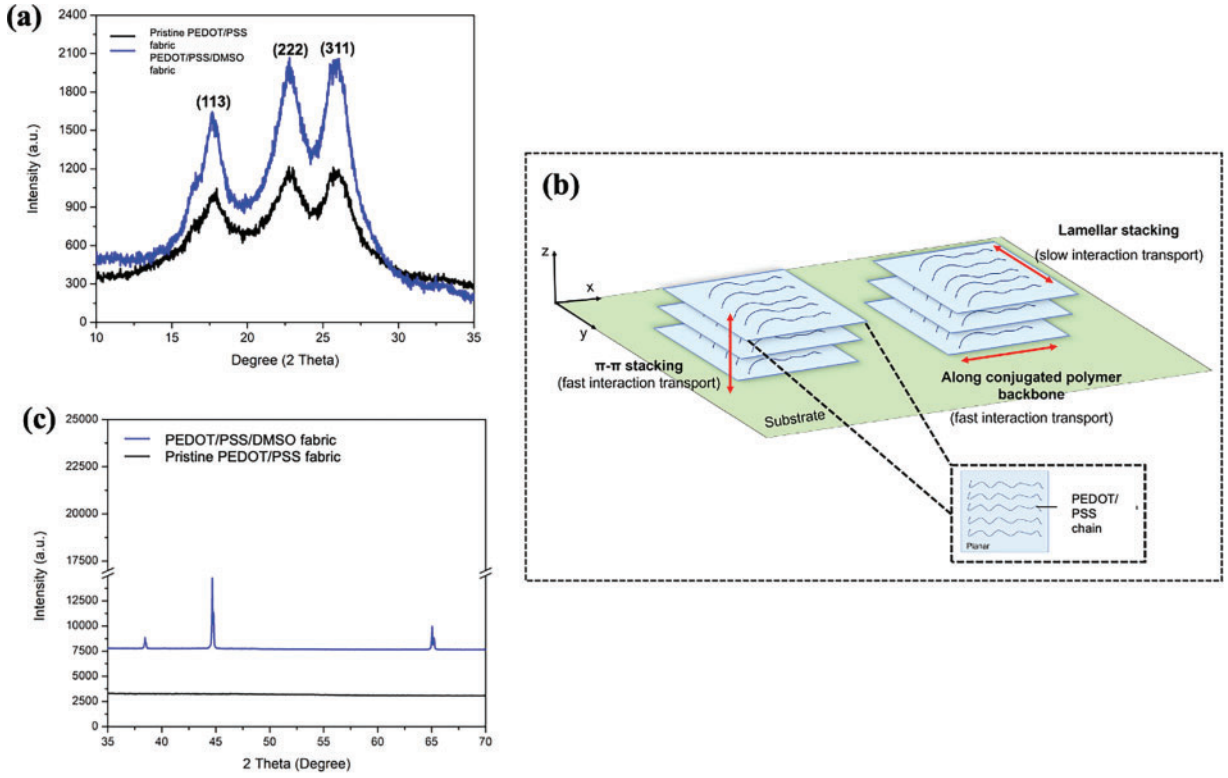

Figure 7: Recorded (a) XRD patterns of pristine PEDOT/PSS fabric and PEDOT/PSS/DMSO fabric. Illustration on (b) the arrangement of π-π stacking, lamellar stacking and conjugated structure of PEDOT/PSS. (c) Crystallinity peak of pristine PEDOT/PSS fabric and PEDOT/PSS/DMSO fabric

Table 4: Crystallinity index of pristine PEDOT/PSS fabric and PEDOT/PSS/DMSO fabric

	Total area of crystalline peak, (A_c)	Total area of crystalline peak, (A_c)	Crystallinity index (%), ($X_c = A_c/A_a$)
Pristine PEDOT/PSS fabric	17,471.16	30,182.34	57.89
PEDOT/PSS/DMSO fabric	22,405.75	33,789.28	66.31

Tensile properties are one of the predominant aspects of developing a durable electronic material. When tensile forces are applied to the fabric, it could constrict its cross-section and extend its length. The maximum breaking force (N) is regarded as the tensile strength, and the elongation (%) is the extension of the fabric under an applied force. PES knitted structure is an anisotropic material in which the yarn is interloped in warp and weft directions. Warp is the lengthwise threads on the fabric to hold the threads in the weft direction stationary (Fig. 8a). Weft direction is the horizontal thread that fills the yarn and contributes to its stretchability (Fig. 8b). The tensile test measured the maximum strength of fabricated PEDOT/PSS fabric in both directions. The data on breaking force and elongation of the fabric is shown in Table 5.

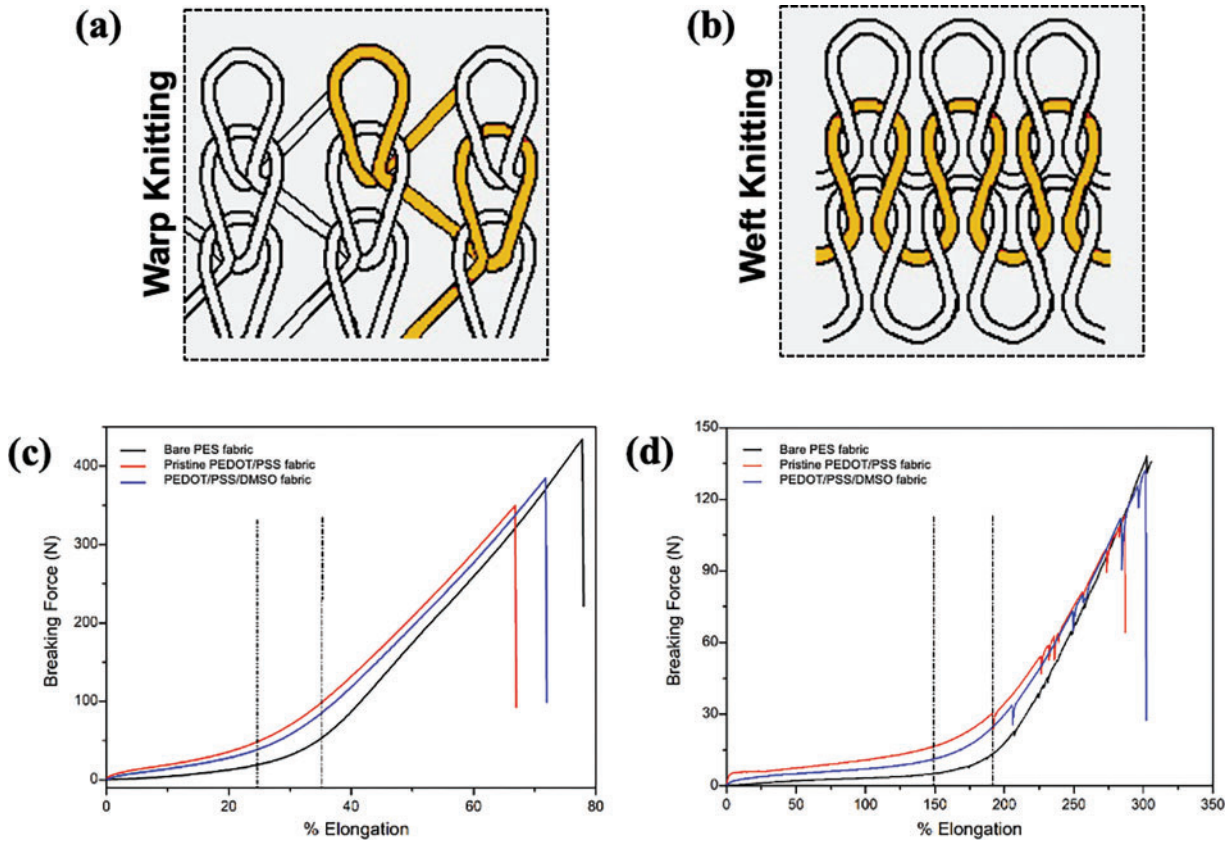

Figure 8: The knitted-PES fabric direction; (a) warp knitting and (b) weft knitting. Tensile strength of bare PES fabric, pristine PEDOT/PSS fabric and PEDOT/PSS/DMSO fabric in (c) warp and (d) weft direction

Table 5: Breaking force (N) and % elongation at break values of the samples

Sample	Breaking force (N)		% Elongation at break	
	Weft	Warp	Weft	Warp
Bare PES fabric	138	434	302	78
Pristine PEDOT/PSS fabric	113	350	287	67
PEDOT/PSS/DMSO fabric	132	385	302	72

Based on the plotted data in Fig. 8c,d, the warp direction produced higher strength compared to the weft direction. For instance, the maximum force for bare PES fabric was 138 and 434 N for weft and warp direction, respectively. In terms of % elongation, the weft offered superior strength, which was at 302% when compared to 78% for warp direction. This data was compared at the graph's first linear region, which corresponded to the fabric's elastic region [73]. During this stage, the loop was stretched within the fabric with an elastic response to the force. Beyond this point, the deformation of loops in the structure of the fabric took place. Smaller slopes were observed in the warp direction. This observation proved that the fabric was less elastic and prone to permanent deformation [74]. The second linear region was also observed in all samples. This linear region was attributed to the stretching of yarns in the structure of loops. Beyond this second linear region, the yarn structure experienced a maximum strength point that led to the failure of the fabric [75].

Interestingly, pristine PEDOT/PSS fabric experienced a drop-in strength and % elongation for both directions. 18% and 19% drop were observed in the maximum force for weft and warp direction, respectively. The fabric became stiffer after being embedded with PEDOT/PSS [22]. The reason behind this phenomenon was potentially due to the phase changes of PEDOT/PSS fabric [76]. Additionally, it could also be generated from the brittleness of PEDOT/PSS as disputed by previous researches [77,78].

In contrast, PEDOT/PSS/DMSO fabric experienced an enhancement of tensile strength of up to 17% (weft). This finding could be credited to the composition of the hard and soft segments in PEDOT/PSS chains. The hard segments provided rigidity, while the soft segments provided elongation [79]. The hard segment was linked along the linear polymer chains in both lateral and directions, forming an efficient cross-linking network that was responsible for the elasticity of the polymer [80]. The presence of DMSO fuelled the transformation of the PEDOT chain from benzoin to quinoid structure, which reinforced the chain rigidity (refer to Fig. 4c). The increased tensile strength of PEDOT/PSS after adding DMSO was due to the attraction of oxygen (O) atom from DMSO to PSSH by hydrogen bonding, which led to the phase separation between PEDOT and PSS [59,81]. Therefore, the strong hydrogen bonding and cohesion of PEDOT grains contributed to the mechanical strength of the overall fabric structure. As a result, PEDOT/PSS/DMSO fabric became stronger with minor deformation.

3.3 Simulated Washing Test

Durability is one of the essential elements in fabricating an innovative fabric. Durability in this study is defined as the ability of the fabric to retain its electrical properties during actual use, such as washing, folding, and rubbing. In this study, the optimized conductivity of the 5 v/v% DMSO/PEDOT fabric from the previous section was tested for durability through simulated washing cycles, and evaluated over a period of up to 30 cycles. The conductivity measurement was recorded in each washing cycle. The results are tabulated in Table S1 and plotted in Fig. 9a.

Fig. 9a shows the conductivity trends of optimised 5v/v% PEDOT/PSS/DMSO fabric during the simulated washing test. A steady drop in the conductivity value was observed up to 10 washing cycles and significantly retained up to 30 washing cycles. During the decrement phase, the discharging effect of PEDOT/PSS molecules from the fabric structure took place. In addition, the utilisation of washing chemicals such as standard soap and mechanical scrubbing also led to the leaching of PEDOT/PSS molecules [82].

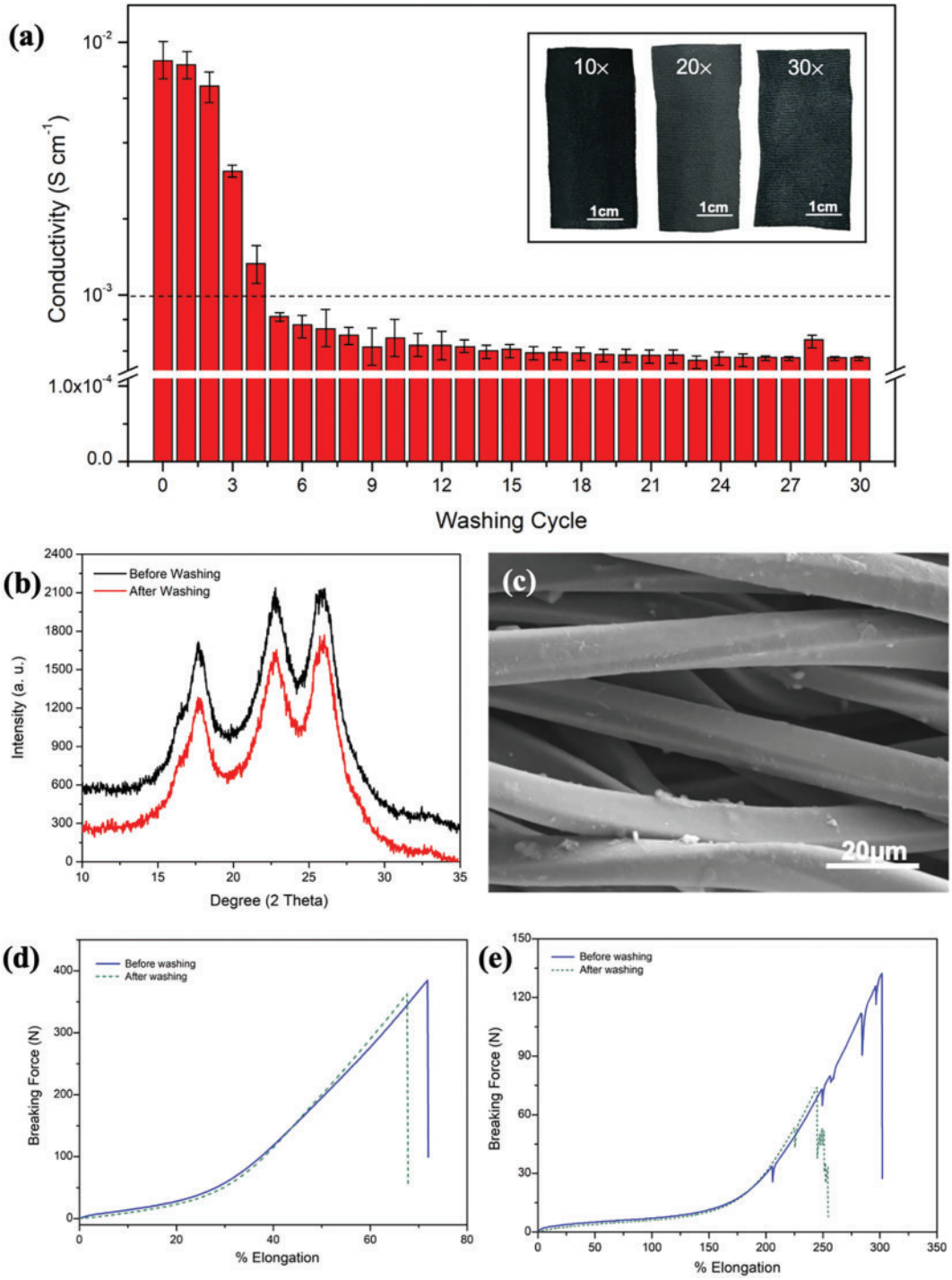

Figure 9: Comparison of (a) conductivity trends of PEDOT/PSS/DMSO fabric over 30 washing cycles. Inset: Physical images of PEDOT/PSS/DMSO fabric in 10, 20 and 30 washing cycles. (b) XRD spectra of PEDOT/PSS/DMSO fabric before and after washing test. (c) Morphological image of PEDOT/PSS/DMSO after washing test. Post-washing tensile of PEDOT/PSS/DMSO fabric in (d) weft and (e) warp directions

After the 10th washing cycle, the conductivity values stabilised. It could be theorised that the conductive network of the PEDOT/PSS/DMSO fabric was able to cope with the washing process. Notably, the conductivity of PEDOT/PSS/DMSO fabric was reduced only by one order of magnitude (10^{-3} to 10^{-4} S cm^{-1}) after 30 washing cycles and maintained its electrical stability at $\sim 5.67 \times 10^{-4}$ S cm^{-1}. However, this decline was still in the acceptable range of conductive state for polymer [59]. During washing, the mechanical stress can cause the PEDOT/PSS to disintegrate, which can reduce its electrical conductivity and cause the fabric to appear paler color (inset Fig. 9a). The crystallinity of PEDOT/PSS/DMSO fabric was further investigated after the washing test. XRD spectrum revealed nochange in the absorption peak position in the post-washing test (Fig. 9b). Nevertheless, a difference in peak intensity at $2\theta = 36.7°$ and 44.0° was found. The crystallinity index dropped by 6% from 66.31% to 62.32% of the crystallinity index. However, this condition was not likely to impart the crystallinity of PEDOT/PSS chains and suggested that the crystallinity of the PEDOT/PSS was maintained after washing [82]. SEM analysis was also performed to observe morphological changes. Based on Fig. 9c, some parts of the post-washed fibre portrayed a clear surface. This condition indicated that PEDOT/PSS was partially removed after ten washing cycles. However, some parts of the PEDOT/PSS coating remained on the fibre structure.

The tensile test results revealed a significant decrease in the tensile strength of the post-washed PEDOT/PSS/DMSO fabric, with a reduction of 44% in the weft direction and 5.6% in the warp direction (Fig. 9d,e). Similarly, the conductivity measurements were also conducted during this study. It was found that the decrement of conductivity in one order of magnitude from $8.44 \pm 0.21 \times 10^{-3}$ S cm^{-1} to $5.65 \pm 0.01 \times 10^{-4}$ S cm^{-1} after 30th washing cycles was observed (Fig. 9a). These two occurrences could be explained from the perspective of chain alignment. It can be deduced that the change in conductivity is related to the change in strength of the fabrics, likely due to the disruption of polymer chain alignment caused by the washing process. When the chains are not properly aligned, the free movement of electrons is impeded, resulting in decreased conductivity [50].

Several factors have influenced the outcomes observed in this study. Among them are mechanical abrasion, chemical action, and the temperature during the washing test. These factors caused dimension instability and fabric distortion, which, in turn, compromised the mechanical properties of the fabric [83]. The impact of these mechanical deformations was evident in the reduced conductivity of the PEDOT/PSS fabric. To improve the fabric's resilience and performance in wearable electronic devices and related fields, it is crucial for future research to explore the relationship between tensile strain and the conductivity of PEDOT/PSS fabric for every washing cycle. By doing this, a deeper understanding of the fabric's behavior in the real washing environment under mechanical stress can be gained, leading to the development of strategies for enhancing its performance.

The retention of conductivity in 30 washing cycles or more is crucial for the durability and practicality of conductive fabric [84,85]. In wearable applications, consistent electrical performance is essential, as repeated washing can degrade the conductive elements within the fabric, potentially rendering the material less functional. Fabrics that retain a significant portion of their initial conductivity, typically 80% or more, after multiple washes are considered viable for long-term use in applications like health monitoring, smart clothing, and energy harvesting [86]. For example, maintaining conductivity is especially significant for health monitoring systems, where sensors embedded in fabrics track physiological parameters like heart rate or respiration [87]. Inaccurate or degraded conductivity can lead to faulty readings or malfunctions, impacting the reliability of these systems. Similarly, for smart clothing used in sports or energy-harvesting textiles, any loss of conductivity could reduce performance, leading to inefficiencies or incorrect data collection [88]. Research has shown that fabrics coated with conductive polymers or silver nanowires retain a high level of conductivity even after numerous wash cycles, with studies reporting less than a 10% reduction in conductivity after 50 washes [89]. In this study, the ability to maintain conductivity after 30 washes underscores the practicality

of these materials for wearable electronics, where both longevity and reliability are critical for their success.

4 Conclusion

This study successfully optimised the dopant concentration of electrically conductive PEDOT/PSS-based fabric to achieve a conductivity value of $8.44 \pm 0.21 \times 10^{-3}$ S cm^{-1} with an optimum concentration of 5% DMSO. This value was tuned to fit within the conductivity range for wearable electronic applications. Prior to this, PEDOT/PSS was synthesised through chemical oxidation and then fabricated into fabric via immersion method. A simulated washing test of up to 30 washing cycles was performed to determine the durability of PEDOT/PSS/DMSO fabric. Even though the conductivity dropped by one order of magnitude (10^{-3} to 10^{-4} S cm^{-1}) after the 5th washing cycle, it continued to maintain its electrical stability at $\sim 5.67 \pm 0.05 \times 10^{-4}$ S cm^{-1} beyond 30 washing cycles. These findings suggest that the conductivity of PEDOT/PSS fabric is stable in the range of polymer materials' conductive states and reveals its good durability for real-world applications in wearable electronics.

Acknowledgement: Authors gratefully thank to the Advanced Polymeric Science Laboratory at the Faculty of Applied Sciences, Universiti Teknologi MARA, Malaysia and the SmartNanoSolution Group located at Qatar University for their invaluable support throughout the research.

Funding Statement: The authors gratefully acknowledge financial support from Universiti Teknologi MARA (UiTM), Malaysia: 600-RMC/GPK 5/3 (177/2020)—Revealing the Mechanism of Electronic Conduction of Polyaniline Fabrics by XPS.

Author Contributions: Conceptualisation, methodology, investigation (polymerisation, fabrication and characterizations), visualisation and original draft preparation: Muhammad Faiz Aizamddin, Nazreen Che Roslan and Ayu Natasha Ayub. Methodology and validation: Muhammad Faiz Aizamddin and Mohamad Arif Kasri. Reviewing and editing: Awis Sukarni Mohmad Sabere, Zarif Mohamed Sofian, Yee Hui Robin Chang, Mohd Ifwat Mohd Ghazali and Muhamad Saipul Fakir. Supervision, reviewing, editing, funding acquisition: Kishor Kumar Sadasivuni and Mohd Muzamir Mahat. All authors reviewed the results and approved the final version of the manuscript.

Availability of Data and Materials: The data that support the findings of this study are available from the corresponding author upon reasonable request.

Ethics Approval: Not applicable.

Conflicts of Interest: The authors declare no conflicts of interest to report regarding the present study.

Supplementary Materials: Supplementary material is available online at https://doi.org/10.32604/jpm.2024.057420.

References

1. Nelson BW, Low CA, Jacobson N, Areán P, Torous J, Allen NB. Guidelines for wrist-worn consumer wearable assessment of heart rate in biobehavioral research. npj Digit Med. 2020;3(1):1–9. doi:10.1038/s41746-020-0297-4.
2. Chander H, Burch RF, Talegaonkar P, Saucier D, Luczak T, Ball JE, et al. Wearable stretch sensors for human movement monitoring and fall detection in ergonomics. Int J Environ Res Public Health. 2020;17(1):1–18. doi:10.3390/ijerph17103554.

3. Arakawa T. Recent research and developing trends of wearable sensors for detecting blood pressure. Sensors. 2018;18(1):2772. doi:10.3390/s18092772.
4. Tran VT, Riveros C, Ravaud P. Patients' views of wearable devices and AI in healthcare: findings from the ComPaRe e-cohort. npj Digit Med. 2019;2(1):1–8. doi:10.1038/s41746-019-0132-y.
5. Rodrigues D, Barbosa AI, Rebelo R, Kwon IK, Reis RL, Correlo VM. Skin-integrated wearable systems and implantable biosensors: a comprehensive review. Biosensors. 2020;10(1):79. doi:10.3390/BIOS10070079.
6. Liu J, Liu M, Bai Y, Zhang J, Liu H, Zhu W. Recent progress in flexible wearable sensors for vital sign monitoring. Sensors. 2020;2(1):1–26. doi:10.3390/s20144009.
7. Tan C, Dong Z, Li Y, Zhao H, Huang X, Zhou Z, et al. A high-performance wearable strain sensor with advanced thermal management for motion monitoring. Nat Commun. 2020;11(1):1–10. doi:10.1038/s41467-020-17301-6.
8. Lund A, Wu Y, Fenech-Salerno B, Torrisi F, Carmichael TB, Müller C. Conducting materials as building blocks for electronic textiles. MRS Bull. 2021;46(1):491–501. doi:10.1557/s43577-021-00117-0.
9. Abdi B, Tarhini A, Baniasadi H, Tehrani-Bagha AR. Developing graphene-based conductive textiles using different coating methods. Adv Mat Tech. 2024;9(4):2301492. doi:10.1002/admt.202301492.
10. Tortosa C, Navarro-Segarra M, Guerrero P, de la Caba K, Esquivel JP. Conductive carbon fabric generation from single-step upcycling of textile waste. Sustain Energy Fuels. 2024;8(1):3844–53. doi:10.1039/D3SE01722B.
11. Zhou S, Zhang C, Fu Z, Zhu Q, Zhou Z, Gong J, et al. Color construction of multi-colored carbon fibers using glucose. Nat Commun. 2024;15(1):1979. doi:10.1038/s41467-024-46395-5.
12. Aizamddin MF, Mahat MM, Nawawi MA, Jani NA, Ariffin ZZ, Yahya SYS. Electrical conductivity and thermal stability of conductive polyaniline fabric-based polyacrylonitrile blends. In: AIP Conference Proceedings, 2023; Yogyakarta, Indonesia.
13. Mahat MM, Sabere ASM, Azizi J, Amdan NAN. Potential applications of conducting polymers to reduce secondary bacterial infections among COVID-19 patients: a review. Emerg Mat. 2021;4(1):279–92.
14. Omar SNI, Ariffin ZZ, Zakaria A, Safian MF, Halim MIA, Ramli R, et al. Electrically conductive fabric coated with polyaniline: physicochemical characterisation and antibacterial assessment. Emergent Mater. 2020;3(1):469–77. doi:10.1007/s42247-019-00062-4.
15. Aizamddin MF, Roslan NC, Kamarudin MA, Omar SNI, Safian MF, Halim MIA, et al. Study of conductivity and thermal properties of polyaniline doped with *p*-toluene sulfonic acid. Malay J Analy Sci. 2020;24(1):413–21.
16. Roslan NC, Aizamddin MF, Omar SNI, Jani NA, Halim MIA, Ariffin ZZ, et al. Morphological and conductivity studies of polyaniline fabric doped phosphoric acid. Malay J Analy Sci. 2020;24(1):698–706.
17. Mahat MM, Aizamddin MF, Roslan NC, Kamarudin MA, Nurzatul S, Omar I, et al. Conductivity, morphology and thermal studies of polyaniline fabrics. J Mech Eng. 2020;9(1):137–50.
18. Lee S. Polypyrrole-wool composite with electrical heating properties fabricated via layer-by-layer method. Sci Rep. 2024;14(1):3883.
19. Aizamddin MF, Shaffee SNA, Halizan MZM, Shafiee SA, Sabere ASM, Sofian ZM, et al. Utilizing membrane technologies in advancing the recycling of spent lithium-ion batteries using green electrochemical method—a review. Mat Res Proceed. 2023;29(1):170–91. doi:10.21741/9781644902516-21.
20. Aizamddin MF, Mahat MM, Ariffin ZZ, Nawawi MA, Jani NA, Amdan NAN, et al. Antibacterial performance of protonated polyaniline-integrated polyester fabrics. Polymers. 2022;14(1):2617. doi:10.3390/polym14132617.
21. Asri NAN, Mahat MM, Zakaria A, Safian MF, Abd Hamid UM. Fabrication methods of electroactive scaffold-based conducting polymers for tissue engineering application: a review. Front Bioeng Biotech. 2022;10:876696. doi:10.3389/fbioe.2022.876696.
22. Tseghai GB, Mengistie DA, Malengier B, Fante KA, van Langenhove L. PEDOT: PSS-based conductive textiles and their applications. Sensors. 2020;20(1):1–18. doi:10.3390/s20071881.
23. Pathak CS, Singh JP, Singh R. Effect of dimethyl sulfoxide on the electrical properties of PEDOT: PSS/n-Si heterojunction diodes. Current App Phys. 2015;15(1):528–34. doi:10.1016/j.cap.2015.01.020.
24. Kim SH, Seong JH, Oh KW. Effect of dopant mixture on the conductivity and thermal stability of polyaniline/nomex conductive fabric. J Appl Polym Sci. 2002;83(1):2245–54. doi:10.1002/app.10211.

25. Alamer FA, Badawi NM, Alodhayb A, Okasha RM, Kattan NA. Effect of dopant on the conductivity and stability of three different cotton fabrics impregnated with PEDOT: PSS. Cellulose. 2020;27(1):531–43. doi:10.1007/s10570-019-02787-1.
26. Le TH, Kim Y, Yoon H. Electrical and electrochemical properties of conducting polymers. Polymers. 2017;4(1):150. doi:10.3390/polym9040150.
27. Cherenack K, Van Pieterson L. Smart textiles: challenges and opportunities. J Appl Phys. 2012;112(1):91301. doi:10.1063/1.4742728.
28. Das SC, Chowdhury N. Smart textiles—new possibilities in textile engineering. IOSR J Polym Text Eng. 2013;1(1):1–6.
29. Sakunpongpitiporn P, Phasuksom K, Paradee N, Sirivat A. Facile synthesis of highly conductive PEDOT: PSS: via surfactant templates. RSC Adv. 2019;9(11):6363–78. doi:10.1039/c8ra08801b.
30. Aizamddin MF, Mahat MM, Nawawi MA. Morphological, structural and electrochemical studies of conductive polyaniline coated polyester fabrics. Int Exc Inn Conf Eng Sci. 2019;5(1):53–7. doi:10.15017/2552935.
31. Aizamddin MF, Mahat MM, Ariffin ZZ, Samsudin I, Razali MSM, Abid Amir M. Synthesis, characterisation and antibacterial properties of silicone-silver thin film for the potential of medical device applications. Polymers. 2021;13(1):3822. doi:10.3390/polym13213822.
32. Kim SM, Kim CH, Kim Y, Kim N, Lee WJ, Lee EH, et al. Influence of PEDOT: PSS crystallinity and composition on electrochemical transistor performance and long-term stability. Nat Commun. 2018;9(1):3858. doi:10.1038/s41467-018-06084-6.
33. Wen Y, Xu J. Scientific importance of water-processable PEDOT-PSS and preparation, challenge and new application in sensors of its film electrode: a review. J Polym Sci A Polym Chem. 2017;55(1):1121–50. doi:10.1002/pola.28482.
34. Gangopadhyay R, Das B, Molla MR. How does PEDOT combine with PSS? Insights from structural studies. RSC Adv. 2014;4(1):43912–20. doi:10.1039/c4ra08666j.
35. Hu L, Song J, Yin X, Su Z, Li Z. Research progress on polymer solar cells based on PEDOT: PSS electrodes. Polymers. 2020;12(1):145. doi:10.3390/polym12010145.
36. Alemu D, Wei HY, Ho KC, Chu CW. Highly conductive PEDOT: PSS electrode by simple film treatment with methanol for ITO-free polymer solar cells. Energy Environ Sci. 2012;5(1):9662–71. doi:10.1039/c2ee22595f.
37. Roslan NC, Aizamddin MF, Ruzaidi DAA, Ayub AN, Asri NAN, Jani NA, et al. Conducting polymer-based textile materials. In: Conjugated polymers for next-generation applications. Elsevier, Woodhead Publishing; 2022. vol. 1, p. 325–59. doi:10.1016/B978-0-12-823442-6.00012-X
38. Teo MY, Kim N, Kee S, Kim BS, Kim G, Hong S, et al. Highly stretchable and highly conductive PEDOT: PSS/Ionic liquid composite transparent electrodes for solution-processed stretchable electronics. ACS Appl Mater Interfaces. 2017;9(1):819–26. doi:10.1021/acsami.6b11988.
39. Ahmad Z, Azman AW, Buys YF, Sarifuddin N. Mechanisms for doped PEDOT: PSS electrical conductivity improvement. Mat Adv. 2021;2(22):7118–38.
40. Lee I, Kim GW, Yang M, Kim TS. Simultaneously enhancing the cohesion and electrical conductivity of PEDOT: PSS conductive polymer films using DMSO additives. ACS Appl Mater Interfaces. 2016;8(1):302–10. doi:10.1021/acsami.5b08753.
41. Hosseini E, Kollath VO, Karan K. Karan K. The key mechanism of conductivity in PEDOT: PPSS thin films exposed by anomalous conduction behaviour upon solvent-doping and sulfuric acid post-treatment. J Mater Chem C Mater. 2020;8(1):3982–90. doi:10.1039/c9tc06311k.
42. Gueye MN, Carella A, Faure-Vincent J, Demadrille R, Simonato JP. Progress in understanding structure and transport properties of PEDOT-based materials: a critical review. Prog Mat Sci. 2020;1(108):100616.
43. Zhu Q, Yildirim E, Wang X, Soo XYD, Zheng Y, Tan TL, et al. Improved alignment of PEDOT: PSS induced by in-situ crystallization of "Green" dimethylsulfone molecules to enhance the polymer thermoelectric performance. Front Chem. 2019;7(1):783. doi:10.3389/fchem.2019.00783.
44. Mengistie DA, Ibrahem MA, Wang PC, Chu CW. Highly conductive PEDOT: PSS treated with formic acid for ITO-free polymer solar cells. ACS Appl Mater Interfaces. 2014;6(1):2292–9. doi:10.1021/am405024d.
45. Zhu Z, Liu C, Xu J, Jiang Q, Shi H, Liu E. Improving the electrical conductivity of PEDOT: PSS films by binary secondary doping. Elec Mat Letters. 2016;12(1):54–8. doi:10.1007/s13391-015-5272-x.

46. Xiong S, Zhang L, Lu X. Conductivities enhancement of poly(3,4-ethylenedioxythiophene)/poly(styrene sulfonate) transparent electrodes with diol additives. Polym Bull. 2013;70(1):237–47. doi:10.1007/s00289-012-0833-8.
47. Mozhzhukhina N, Méndez De Leo LP, Calvo EJ. Infrared spectroscopy studies on stability of dimethyl sulfoxide for application in a Li-air battery. J Phys Chem C. 2013;117(1):18375–80. doi:10.1021/jp407221c.
48. Getnet TM, Loghin C, Chen Y, Wang L, Catalin D, Nierstrasz V. Effect of liquid immersion of PEDOT: PSS-coated polyester fabric on surface resistance and wettability. Smart Mat Struc. 2017;26(1):65016. doi:10.1088/1361-665X/aa6f25.
49. Rajak DK, Pagar DD, Menezes PL, Linul E. Fiber-reinforced polymer composites: manufacturing, properties, and applications. Polymers. 2019;11(1):1667. doi:10.3390/polym11101667.
50. Alamer FA, Althagafy K, Alsalmi O, Aldeih A, Alotaiby H, Althebaiti M, et al. Review on PEDOT: PSS-based conductive fabric. ACS Omega. 2022;7(1):35371–86. doi:10.1021/acsomega.2c01834.
51. Levasseur D, Mjejri I, Rolland T, Rougier A. Color tuning by oxide addition in PEDOT: PSS-based electrochromic devices. Polymers. 2019;11(1):1–12. doi:10.3390/polym11010179.
52. Olivares AJ, Cosme I, Sanchez-Vergara ME, Mansurova S, Carrillo JC, Martinez HE, et al. Nanostructural modification of PEDOT: PSS for high charge carrier collection in hybrid frontal interface of solar cells. Polymers. 2019;11(1):1–17. doi:10.3390/polym11061034.
53. Paquin F, Rivnay J, Salleo A, Stingelin N, Silva C. Multi-phase semicrystalline microstructures drive exciton dissociation in neat plastic semiconductors. J Mater Chem C. 2015;3(1):10715–22. doi:10.1039/b000000x.
54. Ouyang J, Xu Q, Chu CW, Yang Y, Li G, Shinar J. On the mechanism of conductivity enhancement in poly(3,4- ethylenedioxythiophene): poly(styrene sulfonate) film through solvent treatment. Polymer. 2004;45(1):8443–50. doi:10.1016/j.polymer.2004.10.001.
55. Abel SB, Frontera E, Acevedo D, Cesar AB. Functionalization of conductive polymers through covalent postmodification. Polymers. 2023;15(1):205. doi:10.3390/polym15010205.
56. Kanjana N, Maiaugree W, Laokul P, Chaiya I, Lunnoo T, Wongjom P, et al. Fly ash boosted electrocatalytic properties of PEDOT: PSS counter electrodes for the triiodide reduction in dye-sensitized solar cells. Sci Rep. 2023;13(1):6012. doi:10.1038/s41598-023-33020-6.
57. Yildirim E, Wu G, Yong X, Tan TL, Zhu Q, Xu J. A theoretical mechanistic study on electrical conductivity enhancement of DMSO treated PEDOT: PSS. J Mater Chem C Mater. 2018;6(1):5122–31. doi:10.1039/c8tc00917a.
58. Grancarić AM, Jerković I, Koncar V, Cochrane C, Kelly FM, Soulat D, et al. Conductive polymers for smart textile applications. J Indust Text. 2018;48(1):612–42. doi:10.1177/1528083717699368.
59. Aizamddin MF, Mahat MM, Roslan NC, Ruzaidi DAA, Ayub AN. Techniques for designing patterned conducting polymers. In: Conjugated polymers for next-generation applications. Elsevier, Woodhead Publishing; 2022. vol. 1, p. 39–77. doi: 10.1016/B978-0-12-823442-6.00016-7.
60. Omar SNI, Ariffin ZZ, Akhir RAM, Shri DNA, Halim MIA, Safian MF, et al. Polyaniline (PANI) fabric doped *p*-toluene sulfonic acid (*p*TSA) with anti-infection properties. Mat Today: Proceed. 2019;16(1):1994–2002. doi:10.1016/j.matpr.2019.06.083.
61. Hebeish A, Farag S, Sharaf S, Shaheen TI. Advancement in conductive cotton fabrics through *in situ* polymerization of polypyrrole-nanocellulose composites. Carbohydr Polym. 2016;151(1):96–102. doi:10.1016/j.carbpol.2016.05.054.
62. Ayub AN, Ismail NA, Aizamddin MF, Bonnia NN, Sulaiman NS, Nadzri NIM, et al. Effects of organic solvent doping on the structural and conductivity properties of PEDOT: PSS fabric. J Phys Conf Ser. 2022;2169(1):012008. doi:10.1088/1742-6596/2169/1/012008.
63. Yeon C, Kim G, Lim JW, Yun SJ. Highly conductive PEDOT: PSS treated by sodium dodecyl sulfate for stretchable fabric heaters. RSC Adv. 2017;7(1):5888–97. doi:10.1039/c6ra24749k.
64. Moraes MR, Alves AC, Toptan F, Martins MS, Vieira EMF, Paleo AJ, et al. Glycerol/PEDOT:PSS coated woven fabric as a flexible heating element on textiles. J Mater Chem C. 2017;5(1):3807–22. doi:10.1039/C7TC00486A.
65. Ruzaidi DA, Maurya MR, Yempally S, Gafoor SA, Geetha M, Roslan NC, et al. Revealing the improved sensitivity of PEDOT: PSS/PVA thin films through secondary doping and their strain sensors application. RSC Adv. 2023;13(12):8202–19.

66. Mahajan MS, Marathe DM, Ghosh SS, Ganesan V, Sali JV. Changes in in-plane electrical conductivity of PEDOT: PSS thin films due to electric field induced dipolar reorientation. RSC Adv. 2015;5(1):86393–401. doi:10.1039/c5ra13610e.
67. Nardes AM, Kemerink M, de Kok MM, Vinken E, Maturova K, Janssen RAJ. Conductivity, work function, and environmental stability of PEDOT: PSS thin films treated with sorbitol. Org Electron. 2008;9(1):727–34. doi:10.1016/j.orgel.2008.05.006.
68. Li X, Liu Y, Shi Z, Li C, Chen G. Influence of draw ratio on the structure and properties of PEDOT-PSS/PAN composite conductive fibers. RSC Adv. 2014;4(1):40385–89. doi:10.1039/c4ra05952b.
69. Lai YY, Huang VH, Lee HT, Yang HR. Stacking principles on π- and lamellar stacking for organic semiconductors evaluated by energy decomposition analysis. ACS Omega. 2018;3(1):18656–62. doi:10.1021/acsomega.8b02713.
70. Kara MOP, Frey MW. Effects of solvents on the morphology and conductivity of poly(3,4-ethylenedioxythiophene): poly(styrenesulfonate) nanofibers. J Appl Polym Sci. 2014;131(1):1–8. doi:10.1002/app.40305.
71. Piro B, Mattana G, Zrig S, Anquetin G, Battaglini N, Capitao D, et al. Fabrication and use of organic electrochemical transistors for sensing of metabolites in aqueous media. App Sci. 2018;8(1):928. doi:10.3390/app8060928.
72. Kamel MM, El Zawahry MM, Helmy H, Eid MA. Improvements in the dyeability of polyester fabrics by atmospheric pressure oxygen plasma treatment. J Text Inst. 2011;102(1):220–31. doi:10.1080/00405001003672366.
73. Penava Ž., Penava DŠ, Miloš L. Experimental and analytical analyses of the knitted fabric off-axes tensile test. Text Res J. 2021;91(1):62–72. doi:10.1177/0040517520933701.
74. Wu L, Zhao F, Xie J, Wu X, Jiang Q, Lin JH. The deformation behaviors and mechanism of weft knitted fabric based on micro-scale virtual fiber model. Int J Mech Sci. 2020;187(1):105929. doi:10.1016/j.ijmecsci.2020.105929.
75. Ghorbani V, Jeddi AAA, Dabiryan H. Theoretical and experimental investigation of tensile properties of net warp-knitted spacer fabrics. J Text Inst. 2020;111(1):518–28. doi:10.1080/00405000.2019.1649579.
76. Sedighi A, Montazer M, Mazinani S. Fabrication of electrically conductive superparamagnetic fabric with microwave attenuation, antibacterial properties and UV protection using PEDOT/magnetite nanoparticles. Mater Des. 2018;160(1):34–47. doi:10.1016/j.matdes.2018.08.046.
77. Yang Y, Deng H, Fu Q. Recent progress on PEDOT: PSS based polymer blends and composites for flexible electronics and thermoelectric devices. Mater Chem Front. 2020;4(1):3130–52. doi:10.1039/d0qm00308e.
78. Taroni PJ, Santagiuliana G, Wan K, Calado P, Qiu M, Zhang H, et al. Toward stretchable self-powered sensors based on the thermoelectric response of PEDOT: PSS/polyurethane blends. Adv Funct Mater. 2018;28(1):1–7. doi:10.1002/adfm.201704285.
79. Wang X, Ge MQ, Feng GY. The effects of DMSO on structure and properties of PVA/PEDOT: PSS blended fiber. Fib Polymers. 2015;16(1):2578–85. doi:10.1007/s12221-015-5616-z.
80. Yeh F, Hsiao BS, Sauer BB, Michel S, Siesler HW. *In-situ* studies of structure development during deformation of a segmented poly(urethane-urea) elastomer. Macromolecules. 2003;36(1):1940–54. doi:10.1021/ma0214456.
81. Sarabia-Riquelme R, Andrews R, Anthony JE, Weisenberger MC. Highly conductive wet-spun PEDOT: PSS fibers for applications in electronic textiles. J Mat Chem C. 2020;8(1):11618–30. doi:10.1039/D0TC02558E.
82. Du Y, Xu J, Wang Y, Lin T. Thermoelectric properties of graphite-PEDOT: PSS coated flexible polyester fabrics. J Mat Sci: Mat Elect. 2017;28(1):5796–801. doi:10.1007/s10854-016-6250-2.
83. Kašiković N, Vladić G, Milić N, Novaković D, Milošević R, Dedijer S. Colour fastness to washing of multi-layered digital prints on textile materials. J Natl Sci Found. 2018;46(1):381–91. doi:10.4038/jnsfsr.v46i3.8489.
84. Aizamddin MF, Mahat MM. Enhancing the washing durability and electrical longevity of conductive polyaniline-grafted polyester fabrics. ACS Omega. 2023;8(41):37936–47. doi:10.1021/acsomega.3c03377.
85. Wu B, Zhang B, Wu J, Wang Z, Ma H, Yu M, et al. Electrical switchability and dry-wash durability of conductive textiles. Sci Rep. 2015;5(1):11255. doi:10.1038/srep11255.

86. Angelucci A, Cavicchioli M, Cintorrino I, Lauricella G, Rossi C, Strati S, et al. Smart textiles and sensorized garments for physiological monitoring: a review of available solutions and techniques. Sensors. 2021;21(3):814. doi:10.3390/s21030814.
87. Erdem A, Eksin E, Senturk H, Yildiz E, Maral M. Recent developments in wearable biosensors for healthcare and biomedical applications. Trends Anal Chem. 2023;171(1):117510. doi:10.1016/j.trac.2023.117510.
88. Shah MA, Pirzada BM, Price G, Shibiru AL, Qurashi A. Applications of nanotechnology in smart textile industry: a critical review. J Adv Res. 2022;38(1):55–75. doi:10.1016/j.jare.2022.01.008.
89. Aizamddin MF, Ariffin ZZ, Amdan NAN, Nawawi MA, Jani NA, Safian MF, et al. Highly durable antibacterial textiles: cross-linked protonated polyaniline-polyacrylic acid with prolonged electrical stability. ACS Omega. 2024;9(22):23303–15. doi:10.1021/acsomega.3c09871.